

Structure and Dynamics of Polymer-Layered Silicate Nanocomposites

Ramanan Krishnamoorti, Richard A. Vaia,[†] and Emmanuel P. Giannelis

Department of Materials Science and Engineering, Cornell University,
Ithaca, New York 14853-1501

Received February 14, 1996. Revised Manuscript Received June 11, 1996[®]

The static and dynamic properties of polymer-layered silicate nanocomposites are discussed in the context of polymers in confined media. Despite the topological constraints imposed by the host lattice, mass transport of the polymer into the silicate layers (at least in the case of essentially non-polar polystyrene) appears to be unhindered and exhibits mobility similar to that of the pure polymer. However, both the local and global dynamics of the polymer in the hybrids are dramatically different from those in the bulk. On a local scale, intercalated polymer chains exhibit higher flexibility along their backbone along with a marked suppression (or even absence) of cooperative dynamics typically associated with the glass transition. On a global scale, relaxation of polymer chains either tethered to or in close proximity (<1 nm as in intercalated hybrids) to the host surface are dramatically altered and parallel those of other intrinsically anisotropic materials such as block copolymers and liquid crystals.

Introduction

Polymer intercalation into layered inorganic solids is a versatile approach to synthesize organic–inorganic molecular hybrids or polymer nanocomposites.¹ Layered hosts include metal chalcogenides, phosphates, complex oxides, oxychlorides, xerogels, and others. The materials design and synthesis exploits the ability to intercalate into the host lattice a wide range of monomers and polymers.^{2–4} In general, two types of hybrids are possible: **intercalated**, in which a single, extended polymer chain is intercalated between the host layers resulting in a well ordered multilayer with alternating polymer/inorganic host layers and a repeat distance of a few nanometers, and **delaminated**, in which the silicate layers (1 nm thick) are exfoliated and dispersed in a continuous polymer matrix.⁵

In the case of mica-type layered silicates we have recently demonstrated that nanocomposites (both intercalated and delaminated) can be synthesized by direct melt intercalation even with high molecular weight polymers.^{6–14} The synthesis method is quite general and is broadly applicable to a range of commodity polymers from essentially nonpolar polystyrene, to weakly polar poly(ethylene terephthalate) to strongly polar nylon. Nanocomposites can, therefore, be processed using currently available techniques such as extrusion, lowering the barrier toward commercialization.

Pristine mica-type layered silicates usually contain hydrated Na⁺ or K⁺ ions.¹⁵ Ion-exchange reactions with cationic surfactants including primary, tertiary, and quaternary ammonium ions render the normally hydrophilic silicate surface organophilic, which makes possible intercalation of many engineering polymers. The role of alkylammonium cations in the organosili-

cates is to lower the surface energy of the inorganic host and improve the wetting characteristics with the polymer. Additionally, the alkyl ammonium cations could provide functional groups that can react with the polymer or initiate polymerization of monomers to improve the strength of the interface between the inorganic and the polymer.^{16–18}

The unprecedented mechanical properties of polymer layered silicate (PLS) nanocomposites were first demonstrated by a group at the Toyota research center in Japan using nylon nanocomposites.^{18–20} They showed that a doubling of the tensile modulus and strength is achieved for nylon-layered silicate nanocomposites containing as little as 2 vol % inorganic. More importantly the heat distortion temperature of the nanocomposites increases by up to 100 °C extending the use of the composite to higher temperature environments, such as automotive under-the-hood parts.

PLS nanocomposites possess several advantages⁵ including (a) they are lighter in weight compared to conventionally filled polymers because high degrees of stiffness and strength are realized with far less high density inorganic material; (b) their mechanical properties are potentially superior to fiber-reinforced polymers because reinforcement from the inorganic layers will occur in two rather than in one dimension without special efforts to laminate the composites, and (c) they exhibit outstanding diffusional barrier properties without requiring a multipolymer layered design, allowing for recycling.

In addition to their potential applications, PLS nanocomposites are unique model systems to study the statics and dynamics of polymers in confined environments. Generally the dynamics and statics of confined polymers are a fundamental aspect of many industrially important fields such as tribology, adhesion, lubrication, sorption, and catalysis. Using both delaminated and intercalated hybrids, the statics and dynamics of polymers confined over distances ranging from the radius

[†] Current Address: Polymer Branch, Materials Directorate, Wright Laboratory, Wright Patterson AFB, Ohio 45433.

[®] Abstract published in *Advance ACS Abstracts*, August 15, 1996.

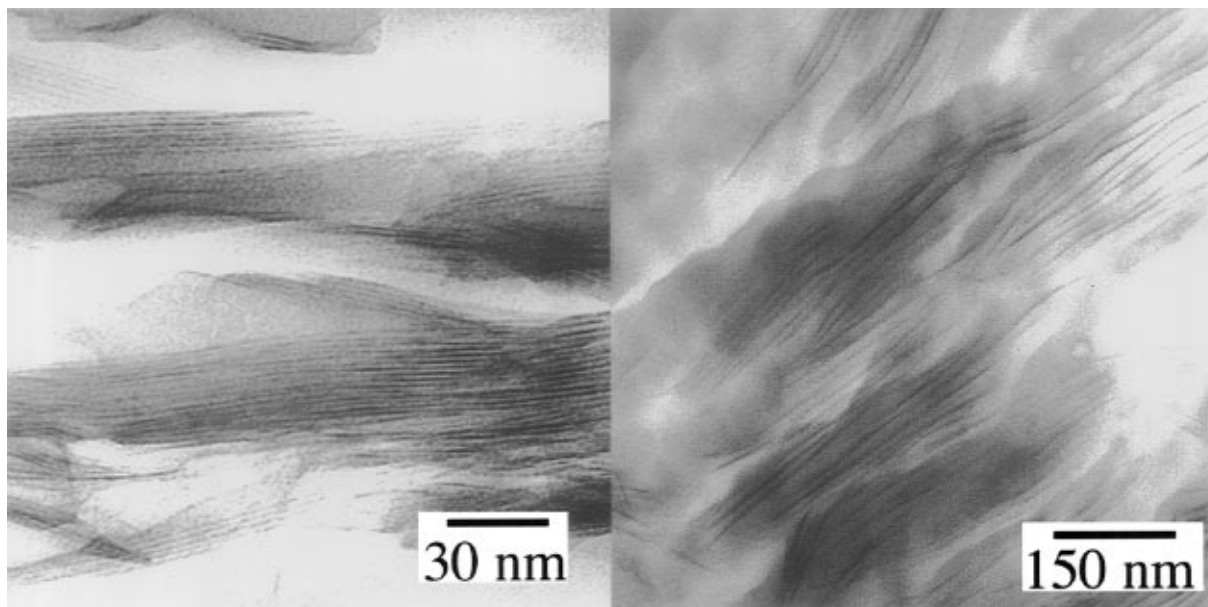


Figure 1. Transmission electron micrographs of (a) an intercalated hybrid of polystyrene and an octadecylammonium-exchanged fluorohectorite (left) and (b) an exfoliated hybrid of bis(2-hydroxyethyl)methyltallow-exchanged montmorillonite with epoxy (right). From refs 11 and 16, respectively.

of gyration of the polymer to the statistical segment length of the chains can be studied.

Even simple notions regarding the conformations of polymers confined to two dimensions are yet to be understood. In three dimensions it is known that for long-chain polymers there is significant overlap between molecules. In two dimensions it has been suggested that different chains should only overlap slightly.²¹ Therefore the local and global conformations of the polymers within the host galleries are expected to be dramatically different from those observed in the bulk not only due to the confinement of the polymer chains but also due to specific polymer–surface interactions, normally not observed in the bulk. It is also expected that the local and chain dynamics would be greatly affected by the confinement as well as the surface–polymer interactions.

In general, the behavior of polymer liquids under confinement is very different from that in the bulk especially when the polymer thickness approaches that of the size of the polymer coil. Traditional notions such as reptation dynamics governing the relaxation of a long polymer chain are improbable in highly confined intercalated systems (confinement distances comparable to the statistical segment length of the polymer) as it is impossible to imagine an entanglement in two dimensions.

In this paper we focus on the dynamics of polymers in intercalated and exfoliated nanocomposites. We start with a brief discussion on the static structure of PLS nanocomposites as revealed by TEM followed by the kinetics of melt-intercalation and conclude with the local (studied by NMR, DSC, and TSC measurements) and global (studied by nanorheology) dynamics of the polymer chains in the nanocomposites.

Structure of PLS Nanocomposites

Structural characterization of PLS nanocomposites has primarily centered around X-ray diffraction and transmission electron microscopy (TEM).^{4,11,16,20} Figure

1a is a TEM bright-field image of an organically modified layered silicate intercalated with polystyrene.¹¹ Individual crystallites of the silicate are visible as regions of alternating narrow, dark and light bands within the particle (fringes). Intercalated hybrids, similar to unintercalated layered silicates, exhibit the microstructure depicted in Figure 1a, with the only difference being an expansion of the gallery height to accommodate the intercalated polymer. Figure 1b shows a section of an exfoliated hybrid wherein individual silicate layers are dispersed in the polymer matrix.¹⁶ The effect of the extremely large aspect ratio of the layers (100–1000) on the relative layer order is demonstrated in the preferential alignment even at these large separations (>10 nm). Additionally, the flexibility of the layers is clearly demonstrated. Even though they are “ceramic” in nature, because of their very large aspect ratio and nanometer thickness, they behave mechanically more like sheets of paper than rigid plates. Similar TEM results have been demonstrated by Lan et al.⁴ and the Toyota group²⁰ using monomer intercalation followed by polymerization.

To obtain more detailed structural information including the conformation of polymer chains and the orientation and arrangement of the host layers, we are currently using small-angle neutron scattering (SANS) on PLS nanocomposites prepared with deuterated polymers. From these experiments, the static structure factor will be obtained for different temperatures and concentrations of labeled species, leading to an accurate determination of the local and global chain conformations of the confined polymers. Previous attempts to determine local structure using X-ray diffraction,^{1c–h,3i,7} have yielded somewhat ambiguous results owing to the constraints imposed by the limited contrast between the host and the polymer.

Kinetics of Formation of PLS Nanocomposites

The observation that polymer chains can undergo center of mass transport in essentially two dimensions

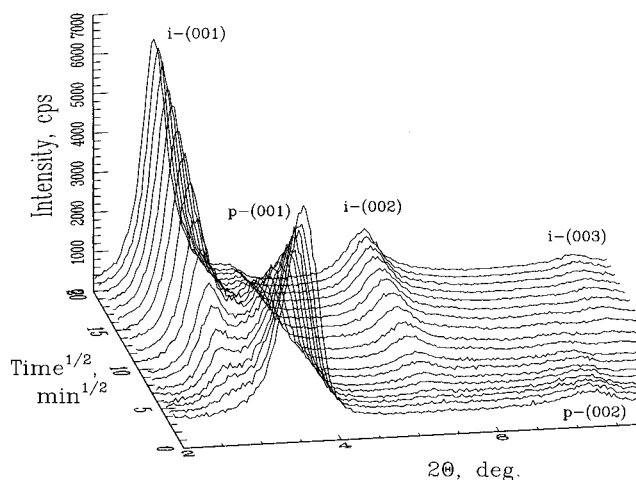


Figure 2. Temporal series of X-ray diffraction patterns for a 30K polystyrene (PS30)/FHC18 mixture annealed in-situ at 160 °C in a vacuum. Initially, basal reflections from the unintercalated FHC18, p-(001) and p-(002), are observed at $2\theta = 4.15$ and $2\theta = 8.03$, respectively, corresponding to a *d* spacing, $d_{001}^p = 2.13$ nm. During the anneal, the intensity of the reflections of the pristine silicate is progressively reduced while a set of new peaks appear corresponding to PS30/FHC18 intercalated hybrid. The *d* spacing for PS30/FHC18 is 3.13 nm. From ref 11.

is rather surprising because the unperturbed radius of gyration of the polymer is roughly an order of magnitude greater than the interlayer distance between the silicate layers.¹¹ The energetic cost of perturbing the chains, in addition to the topographical constraints imposed on the chain motions in a pseudo-two-dimensional slit are expected to impose severe limitations on polymer mobility. The ability for the chains to undergo center of mass transport during melt intercalation is evidence that the interactions within the interlayer *does not* completely restrict segmental motions, otherwise large-scale chain motion would not be possible.

Experimentally it has been observed that the kinetics of intercalation even under quiescent conditions (absence of external shear) are quite rapid. Using in situ X-ray diffraction (which monitors the angular shift and integrated intensity of the silicate reflections) we have studied the kinetics of intercalation of polystyrene into an organically modified layered silicate.¹¹ Figure 2 shows a temporal series of X-ray diffraction patterns for a 30 K polystyrene (PS30)/C18 modified fluorohectorite (FHC18) mixture annealed in situ at 160 °C in vacuum. Details regarding the data collection and analysis are presented in ref 11. The apparent diffusivities for the intercalation of PS30 in FHC18 is the same order of magnitude (10^{-11} cm²/s at 170 °C)¹¹ as the self-diffusion coefficient of polystyrene determined at comparable temperatures and molecular weights.²² Furthermore, the activation energy of melt intercalation is 166 ± 12 kJ/mol which is comparable to the activation energy measured for self-diffusion of polystyrene (167 kJ/mole).²² Polystyrene melt intercalation occurs by mass transport into the host particles and is not specifically limited by diffusion of the polymer chains within the silicate galleries. Additionally, the mobility of the polystyrene chains within the host galleries is at least comparable to that in the melt. Therefore, hybrid formation requires no additional processing time than currently required by conventional polymer-processing techniques such as extrusion.

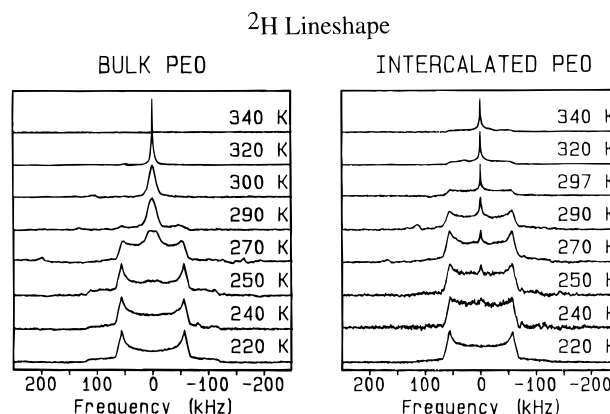


Figure 3. Comparison of ²H NMR line shapes for bulk *d*-PEO and Li-fluorohectorite-intercalated *d*-PEO as a function of temperature. From ref 12.

We are currently using in situ X-ray diffraction along with other microscopic probes of diffusion such as TEM, Rutherford back scattering (RBS), and forward recoil elastic spectroscopy (FRES) to examine the diffusion of more strongly polar polymers, such as poly(2-vinylpyridine) and block copolymers of polystyrene and poly(2-vinylpyridine) and polystyrene and poly(1,4-isoprene) to identify the role of surface–polymer interaction on the kinetics of mass transport as well as on the chain dynamics within the confines of the host layers.

Dynamics of Intercalated Hybrids

Intercalated compounds offer a unique avenue for studying the properties of small molecules and macromolecules in a confined environment. More specifically, layered nanocomposites, because of their nanoscale structure, are ideal model systems to study polymer dynamics in restrictive environments with conventional analytical techniques, such as thermal analysis, NMR, and dielectric spectroscopy. Understanding the changes in the dynamics due to this extreme confinement (layer spacing $\ll R_g$ and comparable to the statistical segment length of the polymer) would provide complementary information to those obtained from traditional surface–force apparatus measurements on confined polymers (confinement distances comparable to R_g).²³

Local Chain Dynamics NMR. The local dynamics of intercalated chains of poly(ethylene oxide) (PEO) were probed using solid-state NMR.¹² Figure 3 compares the ²H line shapes for bulk *d*-PEO and intercalated *d*-PEO (in Li-fluorohectorite), wherein the *d*-PEO chains ($M_w = 180\,000$, $M_w/M_n = 1.2$, Polysciences) are confined to a 0.8 nm gap between the silicate layers.^{6,12} At low temperatures, where the local segmental motion of the polymer is quiescent, a typical powder pattern is observed for both the bulk *d*-PEO and the intercalated *d*-PEO, indicating the spatial motion of the deuterium is slower than the time scale of the experiment (microseconds). However, as the temperature increases, a central peak develops at lower temperatures in the intercalated *d*-PEO than in the bulk *d*-PEO. Additionally, the breadth of the central peak from the intercalated *d*-PEO is substantially narrower than that from the bulk *d*-PEO. This central peak results from increased segmental motion which causes temporal averaging of the signal. The temperature dependence of the line shapes indicates that the intercalated chains

have more "freedom" to sample a distribution of local chain configurations, resulting in increased signal averaging. However, at the highest temperatures, the intercalated *d*-PEO still exhibits a broad base structure reminiscent of the powder pattern whereas the bulk *d*-PEO shows complete motional narrowing of the signal. This indicates that even though the local segmental motion of the intercalated *d*-PEO appears more dynamic at lower temperatures, the silicate layers still restrict motion such that some local configurations of the chain are not accessible, and thus complete signal averaging is not possible.

The enhanced local chain dynamics of the intercalated *d*-PEO reflect the absence of chain entanglements and the presence of excess free volume associated with the packing constraints of intercalated chains. On average, the constraints to local chain dynamics on the length scale of a few monomers are less than the complementary chain in the bulk. However, constraints to local chain motion are not wholly absent as indicated by the residual powder pattern at elevated temperatures. On the basis of geometrical considerations of the extremely narrow 0.8 nm interlayer, a large fraction of the intercalated PEO units are in direct contact with the surface of the silicate. Topologically, the surfaces of the opposing silicate layers will restrict the motions of the *d*-PEO chains. In addition, interactions of the relatively polar PEO segments with the polar silicate surfaces as well as with the interlayer cations will bias the local motion of the *d*-PEO chain to certain energetically favorable orientations. Because of the extended pseudo-2D nature of the chain and the absence of chain entanglements, the local dynamics of the intercalated chains may approach that of a single chain with no excluded volume effects.

Computer simulations probing the dynamics of confined oligomers and short polymers have indicated a strong influence of the confining surface on the local mobility of the molecules.²⁴ Two modes are observed in these simulations—the presence of a fast mode corresponding to the "tail" segments far away from the wall and a slow mode (whose slowing down depends on the surface interaction) corresponding to the "train" segments close to the confining surface, in good agreement with the NMR data.

Cooperative Motion: TSC and DSC. The presence of cooperative motion of chain segments along the intercalated polymer chains may be examined using various analytical techniques such as DSC, TSC, and dielectric spectroscopy. For example, poly(ethylene oxide) ($M_w = 100\,000$, $M_w/M_n = 1.10$, Polysciences)/montmorillonite (PEO/MMT) nanocomposites have been studied by differential scanning calorimetry (DSC) and thermally stimulated dielectric depolarization (or thermally stimulated current, TSC).¹³

Initial DSC experiments on an intercalated PEO/MMT hybrid (20 wt % polymer), indicated the **absence** of any thermal transitions corresponding to the glass or the melting transition of PEO. DSC studies of polystyrene intercalated in an organically modified layered silicate (FHC18) also indicated that the intercalated hybrid does not show a thermal transition corresponding to the glass transition of polystyrene over the temperature range of 30–180 °C.²⁵ Similar absence of a glass transition for polystyrene confined to zeolite

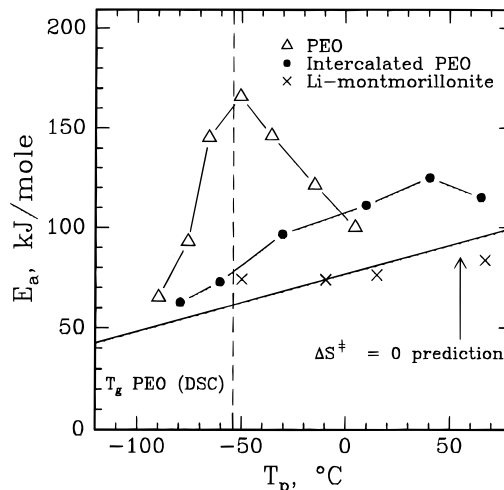


Figure 4. Temperature dependence of the apparent activation energies (E_a) as determined by TSC measurements with thermal sampling for 20 wt % intercalated PEO in montmorillonite, pure PEO and pure montmorillonite (MMT). The departure of E_a from the $\Delta S^\ddagger = 0$ prediction indicates the glass transition region. From ref 13.

cavities has also been observed by Frisch and co-workers.²⁶

In contrast, Keddie et al.²⁷ in their study of thin films of polystyrene on Si(111) found a decrease in T_g for films thinner than 400 Å independent of molecular weight and suggested the presence of a liquidlike layer near the surface of the film. However, in the presence of a strongly interacting surface, the glass transition was found to dramatically increase with decreasing film thickness and was attributed to the presence of a layer close to the surface wherein the mobility is greatly reduced.

Thermally stimulated current techniques have enhanced sensitivity to cooperative relaxations such as glass transitions. To further evaluate the glass transition region of the intercalated PEO, TSC was applied in two modes—"global" and "thermal sampling". Due to the small dipole associated with polystyrene, similar measurements could not be performed with the intercalated polystyrene system. The "global" TSC spectra have some similarity to ac dielectric loss spectra.²⁸ As with DSC, no clear peak was observable in the global TSC spectra of the intercalated PEO in the temperature range of the bulk glass transition for the intercalated PEO. Thus, cooperative relaxations of the intercalated polymer are, at best, weak.

Thermally stimulated current (TSC) measurements with thermal sampling are sensitive to cooperative relaxations from a minor fraction of the overall relaxing species.²⁸ The apparent activation energies, E_a , of relaxations contributing to the depolarization current for 100% PEO, the 20% PEO melt intercalate, and the 0% PEO pressed MMT control pellet are shown in Figure 4. The analysis consists of assigning cooperative glass transition like motions to regions of departure of E_a from the $\Delta S^\ddagger = 0$ prediction.²⁸ For the 20% melt intercalate a distinct peak in E_a is not observed and in fact a broad transition starting at about the nominal PEO T_g and ranging up to about 60 °C is observed.

Since no melting transition was observed in DSC, the fraction of "amorphous" PEO chains in the intercalate is similar to the total PEO content of the hybrids (in

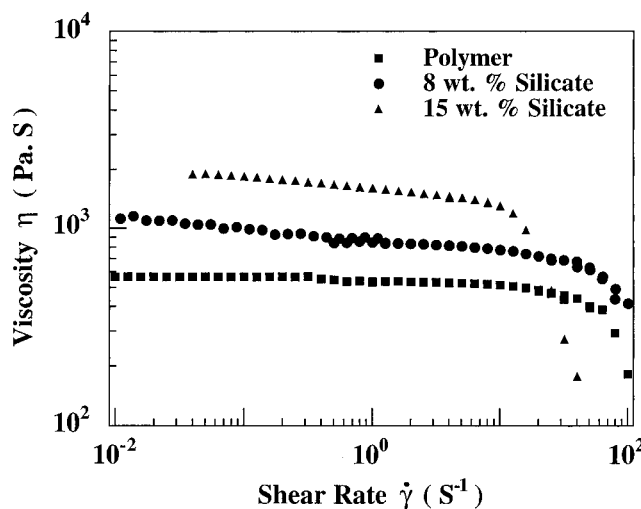


Figure 5. Steady-shear viscosity as a function of shear rate for a series of intercalated hybrids of a copolymer of dimethylsiloxane and diphenylsiloxane with a dimethylditallowmontmorillonite with varying levels of silicate loadings at $T = 28^\circ\text{C}$. The pure polymer exhibits Newtonian behavior at low shear rates and shear thins at high shear rates. The intercalated nanocomposites show an increase in viscosity at all shear rates and exhibit shear thinning at all shear rates accessed in these measurements.

this case $\sim 20\%$). Therefore, the relaxation strength should be at a level where we can easily detect the “cooperative” motions. However, the cooperative relaxations detected in the glass transition region (Figure 4) are weaker than any measured before using the TSC-TS technique. Of the several systems studied with the TSC-TS technique,²⁸ never before has such a broad transition region with a low degree of cooperatively been observed. On the basis of the data in Figure 4, we tentatively conclude that the motions of the intercalated PEO chains are inherently noncooperative relative to the cooperative T_g motions in less unconstrained environments such as the amorphous portion of the bulk polymer or the amorphous chains confined between crystal lamellae in pure semicrystalline PEO. For semi-crystalline PEO, the chains are confined in “amorphous” gaps a few nanometers wide whereas the intercalated PEO occupies a gap of less than 1 nm!

Taken in context with previous investigations of polymer relaxations in confined environments,²⁹ the results from these polymer intercalates appear to indicate that cooperative motion precipitously decreases as polymers are confined to extremely narrow slits less than a few nanometers.

Nanorheology. In this section we present the behavior of PLS nanocomposites subject to a shear flow. Rheology of various nanocomposites—intercalated, exfoliated, and end-tethered exfoliated (prepared by in situ polymerization from reactive groups tethered to the silicate surface), have been performed in a conventional Rheometrics RDA II melt-state rheometer in oscillatory and steady-shear modes.

The steady-shear rheological behavior of a series of intercalated poly(dimethylidiphenyl siloxane) (95–5)-layered silicate (dimethylditallowmontmorillonite) nanocomposites (with varying silicate loadings) are shown in Figure 5.³⁰ The viscosity is enhanced considerably at low shear rates, and increases monotonically with increasing silicate loading (at a fixed shear rate).

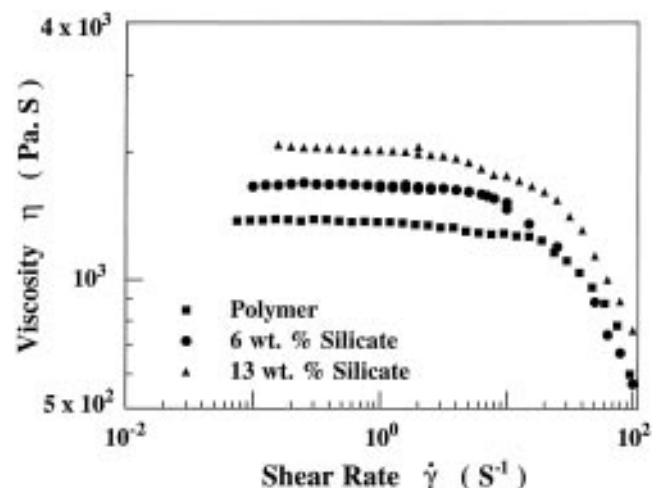


Figure 6. Steady shear viscosity as a function of shear rate for a series of delaminated hybrids of poly(dimethylsiloxane) with dimethylditallowmontmorillonite with varying levels of silicate loadings at $T = 28^\circ\text{C}$. The pure polymer and all the hybrids exhibit Newtonian behavior at low shear rates with enhanced values for the viscosities for the hybrids. With increasing shear rate the polymer and the exfoliated hybrids exhibit shear thinning, with the shear-thinning character setting in at lower shear rates with increasing silicate content.

Furthermore, unlike the polymer wherein a low-shear-rate Newtonian plateau is observed in the viscosity, the intercalated nanocomposites display a shear-thinning behavior at low shear rates. At high shear rates where the polymer displays shear-thinning behavior, the nanocomposites also display shear-thinning with the values of the viscosity (at least at the lower loadings of silicate) being comparable to that of the polymer itself. The same trends are also observable in low-amplitude oscillatory shear measurements of the storage and loss moduli (G' and G'' respectively), wherein a plateau is observed at low frequencies with a concomitant increase (with respect to that of the polymer) in both G' and G'' at all frequencies. It thus appears that the intimate contact between the polymer and the inorganic sheets alters the relaxation dynamics of the polymer, leading to the low-frequency plateau in the moduli and the low-shear-rate non-Newtonian viscosity behavior.

In contrast, for a series of poly(dimethylsiloxane)-based delaminated hybrids (dimethylditallowmontmorillonite), the steady-shear viscosity shows an increase with respect to that of the pure polymer at low shear rates but still obeys Newtonian type behavior, even at the highest silicate loadings examined (Figure 6). The same effect is observed in small-amplitude oscillatory shear measurements, wherein the storage and loss moduli for the delaminated hybrids display similar frequency dependence as the pure polymer, with a monotonic increase in the magnitude of the moduli with increasing silicate loading.³⁰ It thus appears that in these delaminated hybrids, the relaxation of the polymer chains are not altered (at least within the sensitivity of the measurements) by the presence of the silicate layers. This rheological response is similar to the relaxation behavior of typical filled-polymer systems, wherein the relaxation dynamics of the polymer chains are not significantly altered by the presence of the noninteracting filler particles.³¹

We have also studied two delaminated hybrid systems prepared by in situ polymerization—(a) poly(ϵ -caprolac-

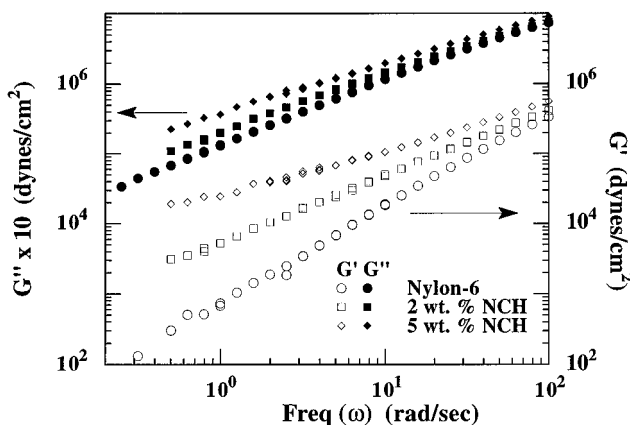


Figure 7. Small strain-amplitude oscillatory shear behavior of nylon-6-montmorillonite end-tethered nanocomposites (NCH) at 235 °C. Storage moduli (G') and loss moduli (G'') as a function of oscillatory frequency (ω) for pure nylon-6, 2 and 5 wt % nanocomposite are shown.

tone)—montmorillonite (PCLC) and (b) nylon-6—montmorillonite (NCH)—herein the polymer chains are end-tethered to the silicate surface via cationic surfactants.³² The small-amplitude oscillatory-shear rheological behavior of these nanocomposites was studied as a function of silicate loading and temperature. For nylon-6-based nanocomposites, the measurements were carried out at a single temperature of 235 °C, and the results are shown in Figure 7. Both G' and G'' show a monotonic increase with increasing silicate loading at all frequencies.

For the molecular weights of the NCH samples examined here, it is expected that at the lower frequencies, the polymer chains should be fully relaxed and exhibit characteristic homopolymer like terminal behavior, i.e., $G' \propto \omega^2$ and $G'' \propto \omega$. While the polydispersity of the polymer chain lengths would affect this behavior, the effect is expected to be small in the dynamic regimes being probed. However, it should be noted that most of the polymer chains in these composites are tethered to the surface at one end and hence cannot relax completely. Terminal zone slopes were estimated for all three samples at frequencies below 10 rad/s, and the frequency dependence of G' decreases monotonically, i.e., going from $\omega^{1.5}$ for nylon-6 to $\omega^{1.0}$ for NCH2 to $\omega^{0.6}$ for NCH5. Also, the frequency dependence of G'' progresses monotonically with silicate loading, i.e., depending as $\omega^{0.95}$ for nylon-6 to $\omega^{0.8}$ for NCH2 to $\omega^{0.7}$ for NCH5. Similar trends were also observed in the PCLC series over a much wider temperature range (55–160 °C), with a saturation in the power-law dependence over 5 wt % silicate and are discussed in more detail in ref 32.

Similar nonterminal low-frequency rheological behavior has been observed in ordered block copolymers and smectic liquid-crystalline small molecules.³³ Several hypotheses have been suggested to explain the observed rheological behavior in these systems.³² We believe that the nonterminal behavior is a result of the end-tethering of the polymers to the layered silicate which arrange themselves as randomly oriented grains (wherein some local order is maintained) with the presence of intergranular defects.

In close analogy to block copolymers and smectic liquid-crystalline small molecules, these nanocomposites can also be aligned using large-amplitude oscillatory

shear. We are currently examining the shear-aligned materials using SAXS and rheological measurements in order to characterize the microstructure of these materials and understand the dynamic processes associated with them.

The end-tethered polymer-layered silicate nanocomposites exhibit a rich variety of rheological properties and can be considered as model systems to examine the rheology of polymer brushes. Understanding the rheological behavior of these systems could elucidate the dynamics of intrinsically anisotropic materials such as block copolymers and liquid-crystalline polymers. Similarities of the rheological response as well as shear-induced ordering of these end-tethered nanocomposites and those of block copolymers and smectic liquid-crystalline polymers are indeed remarkable and illustrate the potential to garner a wealth of information regarding the dynamics of polymer brushes and confined polymers from these simple systems.

Conclusions

PLS nanocomposites offer a unique avenue for studying the static and dynamic properties of confined polymers using conventional analytical techniques usually suitable for bulk samples. The mass transport of polystyrene chains (nearly nonpolar) into the layered silicate appears to be unhindered by the confinement of the chains and exhibits similar diffusion coefficients and temperature dependence of the diffusion coefficient as that in the bulk. However, it is still unclear if this picture would hold true for more strongly interacting polymers and is the subject of ongoing investigations.

The local and global dynamic behavior of confined polymer chains are markedly different from the bulk. Locally, intercalated PEO chains exhibit greater flexibility along the chain backbone and increased free volume as compared to chains in the bulk. Intercalated PS and PEO chains display marked suppression or absence of cooperative dynamics such as exhibited by a glass transition. Intercalated PEO chains do not display a melting transition and behave similar to amorphous chains in the melt even at temperatures significantly below the melting temperature of bulk PEO. On a global scale the relaxation behavior of the polymer chains in the nanocomposites, as detected by conventional rheometry, is dramatically altered when they are tethered to the surface of the silicate or are in close proximity to the silicate layers as in intercalated nanocomposites. Some of these systems show close analogies to other intrinsically anisotropic materials such as block copolymers and smectic liquid-crystalline polymers and can be considered as model systems to understand the dynamics of polymer brushes.

Acknowledgment. This work was supported by the Materials Science Center (MSC) at Cornell University (funded by NSF-DMR-MRSEC) and its Polymer Outreach Program, by WPAFB, and by generous gifts from Amcol, DuPont, Exxon, Hercules, Monsanto, Southern Clay Products, and Xerox. We would like to thank our collaborators Shelly Burnside, Dr. Klaus Jandt, Prof. E. J. Kramer, Dr. W. T. Krawiec, Dr. Evangelos Manias, Prof. P. B. Messersmith, Dr. Brian Sauer, Dr. L. G. Scanlon, Oliver Tse, Dr. Vasudevan, Shan Wong, and Prof. D. B. Zax. We would like to thank Prof. C. C.

Cohen for generous use of the rheometer and Ube Industries for the Nylon nanocomposites. This study benefited from the use of Materials Science Center Facilities at Cornell.

References

- (a) Giannelis, E. P.; Mehrotra, V.; Tse, O. K.; Vaia, R. A.; Sung, T.-C. In *Synthesis and Processing of Ceramics: Scientific Issues*; Rhine, W. E., Shaw, M. T., Gottshall, R. J., Chen, Y., Eds.; MRS Proceedings, Pittsburgh, PA, 1992; pp 249, 547. (b) Wang, M. S.; Pinnavaia, T. J. *Chem. Mater.* **1994**, *6*, 2216. (c) Aranda, P.; Ruiz-Hitzky, E. *Chem. Mater.* **1992**, *4*, 1395. (d) Messersmith, P. B.; Stupp, S. I. *J. Mater. Res.* **1992**, *7*, 2599. (e) Nazar, L. F.; et al. In *Solid State Ionics II*; MRS Proceedings, Pittsburgh, PA, 1991; p 210. (f) Lemmon, J. P.; Lerner, M. M. *Chem. Mater.* **1994**, *6*, 207. (g) Wu, J.; Lerner, M. M. *Chem. Mater.* **1993**, *5*, 835. (h) Ding, Y.; Jones, D. J.; Maireles-Torres, P.; Roziere, J. *Chem. Mater.* **1995**, *7*, 562. (i) Mehrotra, V.; Giannelis, E. P. In *Polymer-Based Molecular Composites*; Shafer, D. W., Mark, J. E., Eds.; MRS Proceedings, Pittsburgh, PA, 1990; p 171. (j) Mehrotra, V.; Giannelis, E. P. *Solid State Commun.* **1991**, *77*, 155. (k) Mehrotra, V.; Giannelis, E. P. *Solid State Ionics* **1992**, *51*, 115.
- (a) Pinnavaia, T. J. *Science* **1983**, *220*, 365. (b) Theng, B. K. G. *The Chemistry of Clay-Organic Reactions*; John Wiley and Sons: New York, 1974. (c) Theng, B. K. G. *Formation and Properties of Clay Polymer Complexes*; Elsevier: New York, 1979. (d) Solomon, D. H.; Hawthorne, D. G. *Chemistry of Pigments and Fillers*; Krieger: Malabar, FL, 1991. (e) Whittingham, M. S.; Jacobson, A. J., Eds. *Intercalation Chemistry*; Academic Press: New York, 1982.
- (a) Cao, G.; Mallouk, T. E. *J. Solid State Chem.* **1991**, *94*, 59. (b) Pillion, J. E.; Thompson, M. E. *Chem. Mater.* **1991**, *3*, 777. (c) Kanatzidis, M. G.; Wu, C.-G.; Marcy, H. O.; DeGroot, D. C.; Kannewurf, C. R. *Chem. Mater.* **1990**, *2*, 222. (d) Liu, Y. J.; DeGroot, D. C.; Schindler, J. L.; Kannewurf, C. R.; Kanatzidis, M. G.; *Chem. Mater.* **1991**, *3*, 992. (e) Kanatzidis, M. G.; Wu, C.-G.; DeGroot, D. C.; Schindler, J. L.; Benz, M.; LeGoff, E.; Kannewurf, C. R. In *NATO ASI Chemical Physics of Intercalation II*; Fisher, J., Ed.; Plenum Press: New York, 1993. (f) Kato, C.; Kuroda, K.; Takahara, H.; *Clays and Clay Miner.* **1981**, *29*, 294. (g) Ogawa, M.; Kuroda, K.; Kato, C.; *Clay Sci.* **1989**, *7*, 243. (h) Fukushima, Y.; Okada, A.; Kawasumi, M.; Kurauchi, T.; Kamigaito, O. *Clay Miner.* **1988**, *23*, 27. (i) Liu, Y.-J.; Schindler, J. L.; DeGroot, D. C.; Kannewurf, C. R.; Hirpo, W.; Kanatzidis, M. G. *Chem. Mater.* **1996**, *8*, 525.
- (4) Lan, T.; Kaviratna, P. D.; Pinnavaia, T. J. *Chem. Mater.* **1995**, *7*, 2144.
- (5) Giannelis, E. P. *Adv. Mater.* **1996**, *8*, 29.
- (6) Vaia, R. A.; Vasudevan, S.; Krawiec, W.; Scanlon, L. G.; Giannelis, E. P. *Adv. Mater.* **1995**, *7*, 154.
- (7) Vaia, R. A.; Ishii, H.; Giannelis, E. P. *Chem. Mater.* **1993**, *5*, 1694. Vaia, R. A. Doctoral Thesis, Cornell University, 1995.
- (8) Vaia, R. A.; Teukolsky, R. K.; Giannelis, E. P. *Chem. Mater.* **1994**, *6*, 1017.
- (9) Burnside, S. D.; Giannelis, E. P. *Chem. Mater.* **1995**, *7*, 1597.
- (10) Vaia, R. A.; Giannelis, E. P. *Macromolecules*, submitted.
- (11) Vaia, R. A.; Jandt, K. D.; Kramer, E. J.; Giannelis, E. P. *Macromolecules* **1995**, *28*, 8080. Vaia, R. A.; Jandt, K. D.; Kramer, E. J.; Giannelis, E. P. *Chem. Mater.*, submitted.
- (12) Wong, S.; Vasudevan, S.; Vaia, R. A.; Giannelis, E. P.; Zax, D. *J. Am. Chem. Soc.* **1995**, *117*, 7568. Wong, S.; Vasudevan, S.; Vaia, R. A.; Giannelis, E. P.; Zax, D. *Solid State Ionics*, in press.
- (13) Vaia, R. A.; Sauer, B. B.; Tse, O. K.; Giannelis, E. P. *J. Polym. Sci., Part B: Polym. Phys.* submitted.
- (14) Krawiec, W.; Scanlon, L. G.; Fellner, J. P.; Vaia, R. A.; Vasudevan, S.; Giannelis, E. P. *J. Power Sources*, in press.
- (15) Brindley, S. W.; Brown, G., Eds. *Crystal Structure of Clay Minerals and their X-ray Diffraction*; Mineralogical Society, London, 1980. Güven, N. In *Hydrous Phyllosilicates*. Bailey, S. W., Ed.; Mineralogical Society of America: Washington, DC, 1988, pp 497–560.
- (16) Messersmith, P. B.; Giannelis, E. P. *Chem. Mater.* **1994**, *6*, 1719.
- (17) Messersmith, P. B.; Giannelis, E. P. *J. Polym. Sci. Part A: Polym. Chem.* **1995**, *33*, 1047.
- (18) Usuki, A.; Kawasumi, M.; Kojima, Y.; Okada, A.; Kurauchi, T.; Kamigaito, O. *J. Mater. Res.* **1993**, *8*, 1174. Usuki, A.; Kojima, Y.; Kawasumi, M.; Okada, A.; Fukushima, Y.; Kurauchi, T.; Kamigaito, O. *J. Mater. Res.* **1993**, *8*, 1179.
- (19) Yano, K.; Usuki, A.; Kurauchi, T.; Kamigaito, O. *J. Polym. Sci., Part A: Polym. Chem.* **1993**, *31*, 2493.
- (20) Kojima, Y.; Usuki, A.; Kawasumi, M.; Okada, A.; Kurauchi, T.; Kamigaito, O. *J. Polym. Sci.: Part A: Polym. Chem.* **1993**, *31*, 983. Kojima, Y.; Usuki, A.; Kawasumi, M.; Okada, A.; Kurauchi, T.; Kamigaito, O.; Kaji, K. *J. Polym. Sci. Part B: Polym. Phys.* **1994**, *32*, 625. Kojima, Y.; Usuki, A.; Kawasumi, M.; Okada, A.; Kurauchi, T.; Kamigaito, O.; Kaji, K. *J. Polym. Sci.: Part B: Polym. Phys.* **1995**, *33*, 1039.
- (21) de Gennes, P. G. *Scaling Concepts in Polymer Physics*; Cornell University Press: Ithaca, NY, 1979.
- (22) Green, P. F.; Kramer, E. J. *J. Mater. Res.* **1986**, *1*, 202. Antonietti, M.; Coutandin, J.; Grütter, R.; Sillescu, R. H. *Macromolecules* **1984**, *17*, 798. Tirrell, M. *Rubber Chem. Technol.* **1984**, *57*, 523.
- (23) Reiter, G. A.; Demirel, L.; Granick, S. *Science* **1994**, *263*, 1741. Overney, R. M. *Trends Polym. Sci.* **1995**, *3*, 359. Pelletier, E.; Montfort, J. P.; Lapique, F. *J. Rheol.* **1994**, *38*, 1151.
- (24) Bitsanis, I. A.; Pan, C. *J. Chem. Phys.* **1993**, *99*, 5520. Mansfield, K. F.; Theodorou, D. N. *Macromolecules* **1989**, *22*, 3143. Manias, E. D. Doctoral Thesis, University of Groningen, 1995.
- (25) In the case of intercalated polystyrene hybrids, the polystyrene was deintercalated and examined using DSC and GPC. The GPC traces before and after were identical, suggesting no degradation or cross-linking. Furthermore, the T_g (a sensitive function of molecular weight in this range) for both pure and deintercalated PS was identical with superimposable DSC traces. On the other hand, PEO undergoes thermal degradation when heated above its melting temperature. Using FTIR, we find that some degradation has taken place in the intercalated PEO samples. Since the techniques used to probe polymer dynamics (NMR, DSC, and TSC) are very localized (<2 –3 nm), the conclusions should be largely unaffected by the slight thermal degradation of PEO.
- (26) Frisch, H. L.; Xue, Y. P. *J. Polym. Sci. Part A: Polym. Chem.* **1995**, *33*, 1979.
- (27) Keddie, J. L.; Jones, R. A. L.; Cory, R. A. *Europhys. Lett.* **1994**, *27*, 59. Keddie, J. L.; Jones, R. A. L.; Cory, R. A. *Faraday Discuss.* **1994**, *98*, 219. Wallace, W. E.; van Zanten, J. H.; Wu, W. *Phys. Rev. E* **1995**, *52*, R3329.
- (28) Sauer, B. B.; Hsiao, B. S. *J. Polym. Sci.: Polym. Phys. Ed.* **1993**, *31*, 917. Sauer, B. B.; DiPaolo, N. V.; Avakian, P.; Kampert, W. G.; Starkweather, H. W. *J. Polym. Sci., Polym. Phys. Ed.* **1993**, *31*, 1851. Sauer, B. B.; Beckerbauer, R.; Wang, L. *J. Polym. Sci., Polym. Phys. Ed.* **1993**, *31*, 1861. Sauer, B. B.; Avakian, P. *Polymer* **1992**, *33*, 5128.
- (29) Cheng, S. Z.; Wu, Z. Q.; Wunderlich, B. *Macromolecules* **1987**, *20*, 2802. Cheng, S. Z.; Cao, M.-Y.; Wunderlich, B. *Macromolecules* **1986**, *19*, 1868.
- (30) Krishnamoorti, R.; Giannelis, E. P. unpublished data.
- (31) Enikolopyan, N. S.; Fridman, M. L.; Stalnova, I. U.; Popov, V. L. *Adv. Polym. Sci.* **1990**, *96*, 1.
- (32) Krishnamoorti, R.; Giannelis, E. P. *Macromolecules*, submitted.
- (33) Rosedale, J. H.; Bates, F. S. *Macromolecules* **1990**, *23*, 2329. Koppi, K. A.; Tirrell, M.; Bates, F. S.; Almdal, K.; Colby, R. H. *J. Phys. II (Paris)* **1993**, *2*, 1941. Larson, R. G.; Winey, K. I.; Patel, S. S.; Watanabe, H.; Bruinsma, R. *Rheol. Acta* **1993**, *32*, 245.

CM960127G